Oriented particles in microwave and submillimeter radiative transfer simulations of ice clouds

Manfred Brath[1], Robin Ekelund[2], Patrick Eriksson[2], Oliver Lemke[1] and Stefan A. Buehler[1]

[1]Universität Hamburg, Faculty of Mathematics, Informatics and Natural Sciences, Department of Earth Sciences, Meteorological Institute, Hamburg, Germany

[2]Department of Space, Earth and Environment, Chalmers University of Technology, Gothenburg, Sweden

May 4, 2020

Contents

Introduction

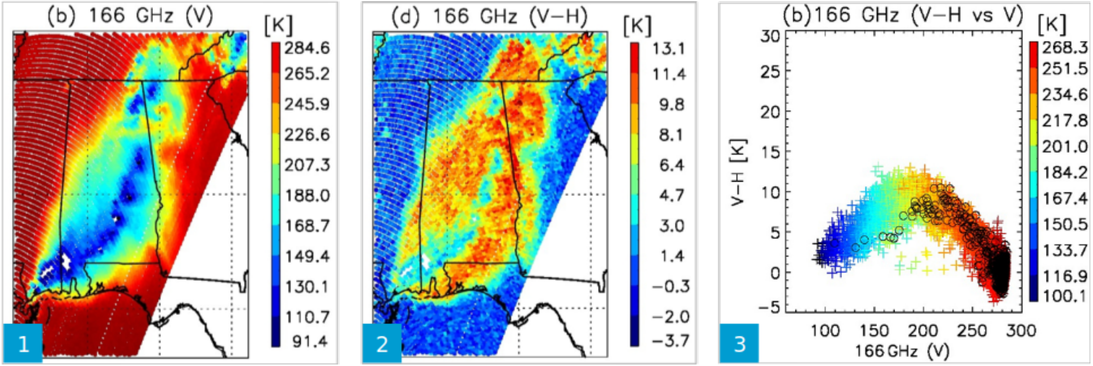

Figure: GMI observed squall line (Southeast U.S., April 29, 2014). 1) shows the vertical polarized brightness temperature and 2) the polarimetric differences. 3) scatter plot for the squall line. Plots taken from Gong and Wu [2017].

- Defer et al. [2014], Gong and Wu [2017] observed polarized cloud signals using satellite borne microwave radiometers.
- These polarized cloud signals cannot be explained by totally randomly oriented particles.
- Conceptual explanation by partially horizontal aligned ellipsoidal ice particles.
- ISMAR (International SubMillimetre Airborne Radiometer) on the FAAM BAe-146 aircraft and ICI (Ice Cloud Imager) on the upcoming MetOp-SG B satellite measure v- and h-polarization at 243 GHz, 664 GHz and 874.4 GHz (planned for ISMAR).
- If we want to exploit these channels, we need consistent scattering data of oriented and more realistic particles for microwave (MW) and submillimeter (SubMM).

Goal

- Scattering of oriented frozen hydrometeors.

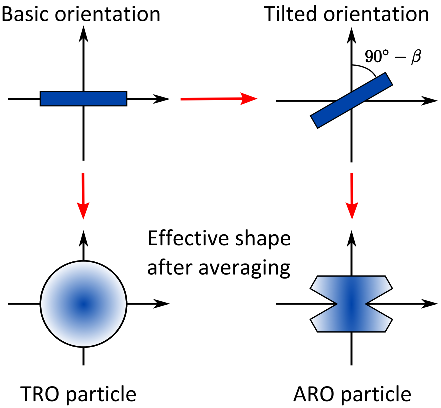

Figure: Schematic of the difference between totally random (TRO) and azimuthally random orientation (ARO).

Total random orientation (TRO)

- Every possible orientation is equally probable and the averaged particle has effectively a spherical symmetry.
- Extinction matrix is constant and scattering matrix depends only on scattering angle.

Azimuthal random orientation (ARO)

- The particle has no preferred azimuthal orientation, but a specific orientation to local zenith (tilt angle β). The averaged particle has effectively a cylindrical symmetry around the z-axis.
- Extinction matrix depends on tilt angle β and incidence polar angle θ_{inc}. Scattering matrix depends on tilt angle, incidence polar angle θ_{inc} and scattering direction (θ_s, ϕ_s).

Existing work

- Scattering databases of Eriksson et al. [2018], Liu [2008] and Hong et al. [2009] cover only total random orientation.
  - Eriksson et al. [2018] valid between 1 GHz and 864 GHz
  - Liu [2008] valid only up to 340 GHz
  - Hong et al. [2009] old refractive index
- Database of Lu et al. [2016] covers orientation of more realistic particles but only up to 94 GHz
- Adams and Bettenhausen [2012] horizontally aligned particles up to 166 GHz

Scattering database

- Scattering calculations done by discrete dipole approximation code ADDA (Yurkin and Hoekstra, 2011) for 32 frequencies between 1 GHz and 886 GHz and 3 temperatures: 190 K, 230 K and 270 K
- Self developed orientation averaging approach
- 2 particle habits: hexagonal plate aggregate (18 sizes between 200 µm and 3.1 mm D_{veq}) and hexagonal plate (51 sizes between 10 µm and 2.5 mm D_{veq})
- Refractive Index: Ice, Mätzler [2006]
- Up to 2562 directions per particle Total calculation time $1.6 \cdot 10^6$ core hours
- Output: scattering matrices $\boldsymbol{Z}$, extinction matrices $\boldsymbol{K}$ and absorption vector $\boldsymbol{a}$ for azimuthally randomly oriented particles with 5° incidence angles spacing and 10° tilt angle spacing
- The scattering database is publicly available from Zenodo (`https://doi.org/10.5281/zenodo.3463003`)
- For details see Brath et al., 2019 (AMT, in press)

Scattering data example I

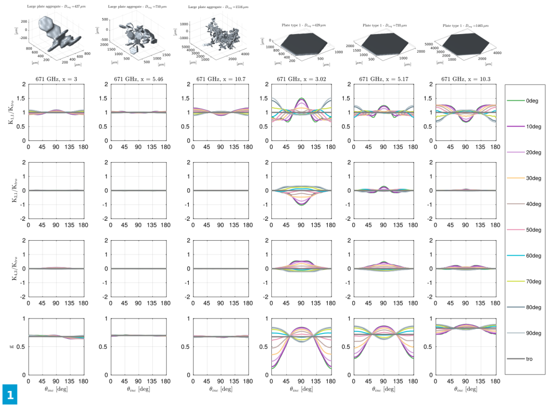

Figure: Extinction matrix elements K_{ij}normalized by the extinction cross section for total random orientation and the asymmetry parameter g of large (hexagonal) plate aggregate and hexagonal plate (plate type 1) for different size parameter x at 671 GHz as function of incidence angle θ_{inc} for several tilt angles β. The gray line denotes total random orientation.

Scattering data example II

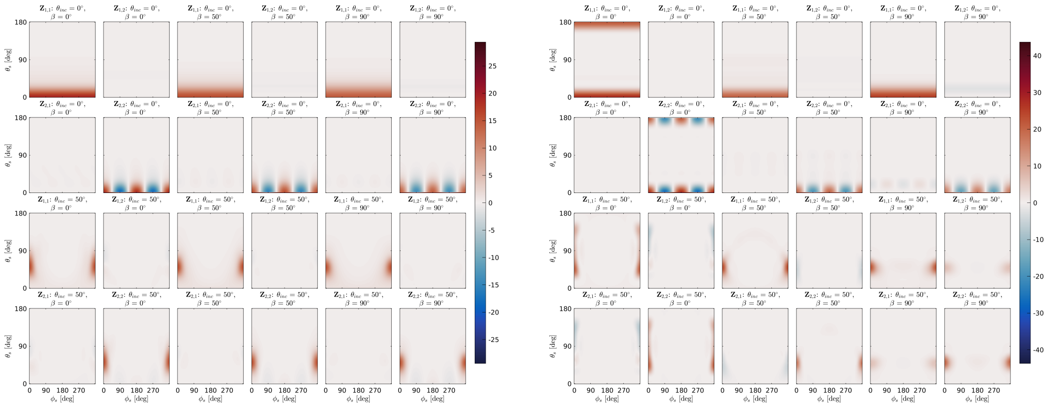

Figure: The upper left block of the phase matrix of large (hexagonal) plate aggregate (right) and hexagonal plate (plate type 1, right) as function of the polar scattering angle θ_s and the azimuth scattering angle ϕ_s for a set of tilt angles β and incidence angles θ_{inc}. Both habits have a volume equivalent diameter of $\approx 430\,\mu m$ (size parameter $x \approx 3$ at 671 GHz).

Radiative transfer simulations

- RT model: Atmospheric Radiative Transfer Simulator (ARTS, Buehler et al., 2018, Eriksson et al., 2011) version 2.3.1118
- Scattering solver: Discrete ordinate iterative (DOIT, Emde, 2004)
- Frequencies: 166, 243, 664 GHz
- Incidence angle: $\approx 50^\circ$ (similar to GMI and ICI)
- Atmospheric data: Transect from Global Environmental Multiscale Model (GEM, Côté et al., 1998)
- 4 frozen (cloud ice, snow, graupel, hail) and 2 liquid hydrometeors (liquid cloud, rain)
- Scattering data except for snow and ice: Eriksson et al. [2018]
- Fluttering snow and ice: 7 different levels of fluttering with zero mean and increasing standard deviation

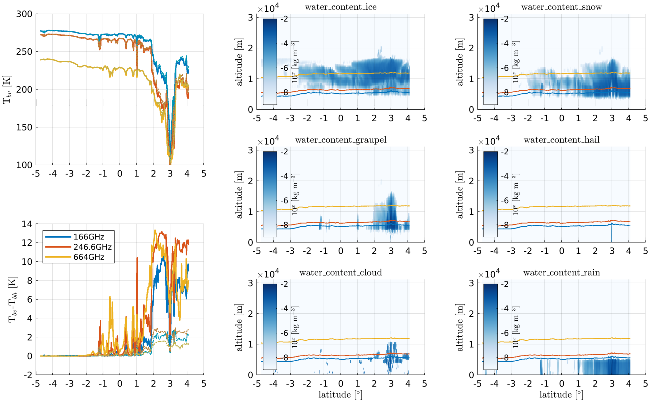

Figure: Simulated transect. (left) simulated brightness temperatures and polarization differences. (mid and right) hydrometeor contents of transect. The lines in the mid and right plots denote the emission heights for corresponding clear sky conditions.

Simulation results: polarization scatter plots (166 GHz)

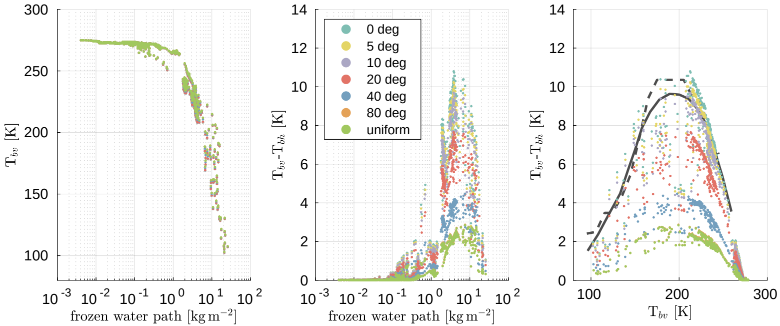

Figure: Simulated brightness temperature at 166 GHz of the transect for azimuthally randomly oriented snow and ice particles orientation averaged over 7 different distributed β angles with zero mean and different standard deviation. The different colors denote the standard deviation of the β angle distribution and the distribution type. The gray line solid line denotes the mean polarization difference over tropical ocean from GMI observations at 166 GHz of Gong and Wu [2017] and the gray dashed line the mean polarization difference over tropical ocean from MADRAS observations at 157 GHz of Defer et al. [2014].

Simulation results: polarization scatter plots (243 GHz and 664 GHz)

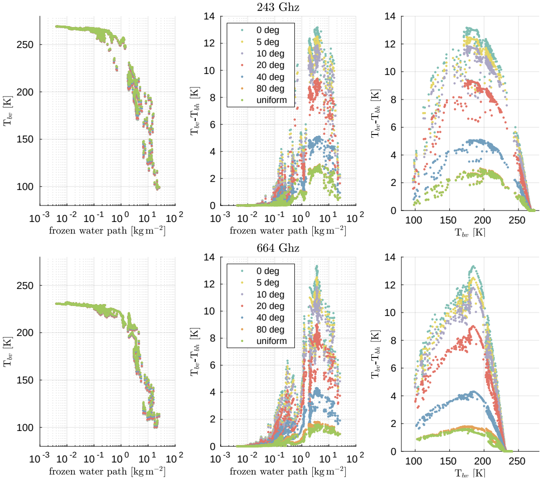

Figure: Similar to slide 16 but now ICI perspective.

Summary

- Provided scattering database for azimuthally randomly oriented hexagonal plate aggregates and hexagonal plates for 32 frequencies between 1 GHz and 886 GHz and 3 temperatures: 190 K, 230 K and 270 K
- The scattering data is publicly available from Zenodo (`https://doi.org/10.5281/zenodo.3463003`)
- Paper about scattering database in press (Brath et al., 2019; AMT)
- Radiative transfer simulations using our database recreate observed polarization pattern

References

I. S. Adams and M. H. Bettenhausen. The scattering properties of horizontally aligned snow crystals and crystal approximations at millimeter wavelengths. *Radio Science*, 47(5), 2012.

S. A. Buehler, J. Mendrok, P. Eriksson, A. Perrin, R. Larsson, and O. Lemke. Arts, the atmospheric radiative transfer simulator – version 2.2, the planetary toolbox edition. *Geoscientific Model Development*, 11(4):1537–1556, 2018. doi: 10.5194/gmd-11-1537-2018. URL https://www.geosci-model-dev.net/11/1537/2018/.

Jean Côté, Sylvie Gravel, André Méthot, Alain Patoine, Michel Roch, and Andrew Staniforth. The Operational CMC-MRB Global Environmental Multiscale (GEM) Model. Part I: Design Considerations and Formulation. *Monthly Weather Review*, 126(6):1373–1395, June 1998. ISSN 0027-0644.

Eric Defer, Victoria S. Galligani, Catherine Prigent, and Carlos Jimenez. First observations of polarized scattering over ice clouds at close-to-millimeter wavelengths (157 GHz) with MADRAS on board the Megha-Tropiques mission. *Journal of Geophysical Research: Atmospheres*, 119(21):2014JD022353, November 2014. ISSN 2169-8996. doi: 10.1002/2014JD022353.

C. Emde. A polarized discrete ordinate scattering model for simulations of limb and nadir long-wave measurements in 1-D/3-D spherical atmospheres. *Journal of Geophysical Research*, 109(D24), 2004. ISSN 0148-0227. doi: 10.1029/2004jd005140.

P. Eriksson, S.A. Buehler, C.P. Davis, C. Emde, and O. Lemke. Arts, the atmospheric radiative transfer simulator, version 2. *Journal of Quantitative Spectroscopy and Radiative Transfer*, 112(10):1551–1558, July 2011. ISSN 0022-4073. doi: 10.1016/j.jqsrt.2011.03.001.

P. Eriksson, R. Ekelund, J. Mendrok, M. Brath, O. Lemke, and S. A. Buehler. A general database of hydrometeor single scattering properties at microwave and sub-millimetre wavelengths. *Earth System Science Data*, 10(3):1301–1326, 2018. doi: 10.5194/essd-10-1301-2018. URL https://www.earth-syst-sci-data.net/10/1301/2018/.

Jie Gong and Dong L Wu. Microphysical properties of frozen particles inferred from global precipitation measurement (gpm) microwave imager (gmi) polarimetric measurements. *Atmospheric Chemistry and Physics*, 17(4):2741–2757, 2017.

Gang Hong, Ping Yang, Bryan A Baum, Andrew J Heymsfield, Fuzhong Weng, Quanhua Liu, Georg Heygster, and Stefan A Buehler. Scattering database in the millimeter and submillimeter wave range of 100–1000 GHz for nonspherical ice particles. *Journal of Geophysical Research: Atmospheres (1984–2012)*, 114(D6), 2009.

Guosheng Liu. A database of microwave single-scattering properties for nonspherical ice particles. *Bulletin of the American Meteorological Society*, 89(10):1563–1570, 2008. doi: 10.1175/2008BAMS2486.1.

Yinghui Lu, Zhiyuan Jiang, Kultegin Aydin, Johannes Verlinde, Eugene E Clothiaux, and Giovanni Botta. A polarimetric scattering database for non-spherical ice particles at microwave wavelengths. *Atmospheric Measurement Techniques*, 9(10):5119–5134, 2016.

Christian Mätzler. *Thermal microwave radiation: applications for remote sensing*, volume 52. IET, 2006.

Maxim A. Yurkin and Alfons G. Hoekstra. The discrete-dipole-approximation code ADDA: Capabilities and known limitations. *Journal of Quantitative Spectroscopy and Radiative Transfer*, 112(13):2234–2247, September 2011. ISSN 0022-4073. doi: 10.1016/j.jqsrt.2011.01.031. URL http://www.sciencedirect.com/science/article/pii/S0022407311000562.